# The Structural Integrity of Lignin Is Crucial for Resistance against *Striga hermonthica* Parasitism in Rice[1[OPEN]]

**J. Musembi Mutuku,[a,2,3] Songkui Cui,[b,c,d,2] Chiaki Hori,[e] Yuri Takeda,[f] Yuki Tobimatsu,[f] Ryo Nakabayashi,[d] Tetsuya Mori,[d] Kazuki Saito,[d,g] Taku Demura,[c] Toshiaki Umezawa,[f,h] Satoko Yoshida,[b,c,d] and Ken Shirasu[d,i,3,4]**

[a]Biosciences Eastern and Central Africa – International Livestock Research Institute (BecA-ILRI) Hub, 00100 Nairobi, Kenya
[b]Institute for Research Initiatives, Division for Research Strategy, Nara Institute of Science and Technology, Ikoma, Nara 630-0192, Japan
[c]Division of Biological Science, Nara Institute of Science and Technology, Ikoma, Nara 630–0192, Japan
[d]RIKEN Center for Sustainable Resource Science, Tsurumi-ku, Yokohama, Kanagawa 230–0045, Japan
[e]Research Faculty of Engineering, Hokkaido University, Sapporo, Hokkaido 060-8628, Japan
[f]Research Institute for Sustainable Humanosphere, Kyoto University, Uji, Kyoto 611-0011, Japan
[g]Graduate School of Pharmaceutical Sciences, Chiba University, Chuo-ku, Chiba 260-8675, Japan
[h]Research Unit for Development and Global Sustainability, Kyoto University, Uji, Kyoto 611-0011, Japan
[i]Graduate School of Biological Sciences, The University of Tokyo, Bunkyo-ku, Tokyo 113-0033, Japan

**ORCID IDs: 0000-0002-3985-368X (J.M.M.); 0000-0001-7777-6681 (S.C.); 0000-0002-7578-7392 (Y.T.); 0000-0002-8674-0928 (R.N.); 0000-0002-2499-4738 (T.D.); 0000-0003-1135-5387 (T.U.); 0000-0002-9999-7861 (S.Y.); 0000-0002-0349-3870 (K.S.).**

*Striga* species are parasitic weeds that seriously constrain the productivity of food staples, including cereals and legumes, in Sub-Saharan Africa and Asia. In eastern and central Africa, *Striga* spp. infest as much as 40 million hectares of smallholder farmland causing total crop failure during severe infestation. As the molecular mechanisms underlying resistance are yet to be elucidated, we undertook a comparative metabolome study using the *Striga*-resistant rice (*Oryza sativa*) cultivar 'Nipponbare' and the susceptible cultivar 'Koshihikari'. We found that a number of metabolites accumulated preferentially in the *Striga*-resistant cultivar upon *Striga hermonthica* infection. Most apparent was increased deposition of lignin, a phenylpropanoid polymer mainly composed of *p*-hydroxyphenyl (H), guaiacyl (G), and syringyl (S) aromatic units, around the site of interaction in Nipponbare. The increased deposition of lignin was accompanied by induction of the expression of corresponding enzyme-encoding genes in the phenylpropanoid pathway. In addition, perturbing normal lignin composition by knocking down or overexpressing the genes that regulate lignin composition, i.e. *p*-COUMARATE 3-HYDROXYLASE or FERULATE 5-HYDROXYLASE, enhanced susceptibility of Nipponbare to *S. hermonthica* infection. These results demonstrate that enhanced lignin deposition and maintenance of the structural integrity of lignin polymers deposited at the infection site are crucial for postattachment resistance against *S. hermonthica*.

Witchweeds (*Striga* spp.) are members of the Orobanchaceae family, which is composed of root parasites and are among the most economically important parasitic plants for modern agriculture globally (Scholes and Press, 2008). In Africa, five of the most economically important *Striga* species, i.e. *Striga hermonthica*, *Striga asiatica*, *Striga forbesii*, *Striga aspera*, and *Striga gesnerioides*, affect the production of sorghum (*Sorghum bicolor*), finger millet (*Eleusine coracana*), maize (*Zea mays*), sugarcane (*Saccharum officinarum*), and cowpea (*Vigna unguiculata*), resulting in annual losses of over 1 billion USD in cereal productivity alone (Spallek et al., 2013; Gobena et al., 2017). The development of resistance in host species remains one of the most efficient and cost-effective ways to control infestations of the parasitic plants (Riches and Parker, 1995). Cultivars and wild relatives of crop species, including sorghum and rice (*Oryza sativa*), that show resistance to *Striga* spp., have been identified (Hess et al., 1992; Gurney et al., 2006; Cissoko et al., 2011; Gobena et al., 2017). For example, rice cultivars, IR47255-B-B-5-4, IR49255-B-B-5-2, Nipponbare, and IR64 have been reported to be *Striga*-resistant (Harahap et al., 1993; Gurney et al., 2006; Yoshida and Shirasu, 2009). In Africa, the NEw RICe for Africa (NERICA) cultivars, which were developed to combine the high yielding characteristics of the Asian rice species *O. sativa* (WAB56-104, WAB56-50, and WAB181-18) with the local stress-resistance abilities of the African species *Oryza glaberrima* (CG14; Jones et al., 1997), have gained prominence. Eighteen interspecific upland cultivars, named NERICA-1 to NERICA-18, are available to rice farmers (Jamil et al., 2011). Some NERICA cultivars (i.e. NERICA-1, NERICA-3, NERICA-4, NERICA-12, and NERICA-17) have been reported to have *Striga* resistance when screened under laboratory conditions (Cissoko et al., 2011), and

 

this resistance was confirmed when these cultivars were exposed to *S. hermonthica* under field conditions (Rodenburg et al., 2015).

The mechanisms of resistance to parasitic plants vary depending on the host species and cultivars (Saucet and Shirasu, 2016). Broadly speaking, two types of resistance against the Orobanchaceae parasitic plants have been reported (i.e. pre- and postattachment resistance; Hess et al., 1992; Gurney et al., 2006; Yoshida and Shirasu, 2009). Preattachment resistance involves the production of lower levels of parasite germination stimulants such as strigolactones by the host (Hess et al., 1992; Matusova et al., 2005; Gobena et al., 2017). On the other hand, postattachment resistance involves strengthening of pre-existing and inducible mechanisms that prevent vascular continuity with the parasite after forming an invasive organ called an "haustorium" (Swarbrick et al., 2008; Li and Timko, 2009; Yoshida and Shirasu, 2009; Yoshida et al., 2016). For example, the penetration of *Orobanche minor* into salicylic-acid–treated red clover (*Trifolium pretense*) stops at the lignified endodermis of the host root, preventing the connection of host and parasite vasculature (Kusumoto et al., 2007). In the case of sunflower (*Helianthus* sp.), a cultivar resistant to *Orobanche cumana* shows enhanced cell wall deposition at the infection site, thereby inhibiting parasite development by causing cellular disorganization of the parasite (Labrousse et al., 2001).

Lignin is an abundant phenylpropanoid polymer constituting the secondary cell wall of vascular plants. The lignin polymer is synthesized via oxidative radical coupling of lignin monomers, mainly of the three types of monolignols (i.e. *p*-coumaryl alcohol, coniferyl alcohol), and sinapyl alcohol, which constitute *p*-hydroxyphenyl (H), guaiacyl (G), and syringyl (S) units in the lignin polymers, respectively; in addition, γ-acylated lignin units arise from incorporation of γ-*p*-coumarylated monolignols during lignification, particularly in grasses (Fig. 1). These lignin monomers, along with many other specialized metabolites such as flavonoids, are derived from the phenylpropanoid pathway (Fig. 1). Notably, the biosynthesis and deposition of lignin or lignin-like phenolic polymers in cell walls can be induced rapidly in response to biotic and abiotic stresses, as well as to structural damage (Humphreys and Chapple, 2002; Caño-Delgado et al., 2003). In particular, various metabolic enzymes in the lignin biosynthesis pathway are required for resistance against various pathogens. For example, in wheat (*Triticum monococcum*), silencing genes encoding the monolignol biosynthesis enzymes, such as Phe ammonia-lyase (PAL), caffeic acid o-methyltransferase (COMT), caffeoyl-CoA o-methyltransferase (CCoAOMT), and cinnamyl alcohol dehydrogenase (CAD), leads to susceptibility of leaf tissues to the fungal pathogen *Blumeria graminis* f. sp. *tritici*, the causal agent of powdery mildew disease (Bhuiyan et al., 2009). In Arabidopsis (*Arabidopsis thaliana*), the *reduced epidermal fluorescence8* mutant, which is defective in the gene encoding *p*-COUMARATE 3-HYDROXYLASE (or *p*-COUMAROYL ESTER 3-HYDROXYLASE [C3′H]) required for the generation of G- and S-lignin polymer units (but not H-units; Fig. 1), accumulates H-enriched lignin polymers in cell walls, and shows increased susceptibility to fungal attack (Franke et al., 2002; Bonawitz et al., 2014). In some cases, however, down-regulation of metabolic enzyme-encoding genes in the phenylpropanoid pathway results in resistance against pathogens. For example, in alfalfa (*Medicago sativa*), down-regulation of the gene encoding hydroxycinnamoyl-CoA shikimate/quinate hydroxycinnamoyl transferase results in the reduction of lignin levels, constitutive defense responses, and enhanced tolerance to the fungal pathogen *Colletotrichum trifolii* (Gallego-Giraldo et al., 2011). Similarly, *COMT* and *CCoAOMT* antisense tobacco (*Nicotiana tabacum*) lines are more resistant to *Agrobacterium tumefaciens* infection as compared to the wild-type plants (Maury et al., 2010). In yet another example, sorghum lines with defective *CAD* and *COMT* genes resulting in an altered lignin content and composition (Oliver et al., 2005), are resistant to *Fusarium* spp. (Funnell-Harris et al., 2010). From these examples, it is possible that enforced alteration of lignin composition may lead to the production of damage-associated molecular patterns, which could enhance resistance to specific pathogen types. However, the impact of lignin modification on the regulation of defense responses is yet to be fully elucidated.

Previous reports demonstrated the existence of differences in susceptibility between the rice cultivar 'Koshihikari' and the rice cultivar 'Nipponbare', upon infection by *S. hermonthica*. Nipponbare often prevents *S. hermonthica* penetration to the endodermis or limits its growth after vascular connection (Gurney et al., 2006; Yoshida and Shirasu, 2009). Nipponbare is not only resistant to parasitism by *Striga* spp. but has

[1]This work was partly supported by the Japan Society for the Promotion of Science (postdoctoral fellowship to J.M.M.), and KAKENHI (grant nos. 17K15142 to S.C., 17J0965416 to Y.Ta., 16K14958 and 16H06198 to Y.To., 24228008, 15H05959, and 17H06172 to K.Sh., and 18H02464 and 18H04838 to S.Y.); the Japan Advanced Plant Science Network, International Atomic Energy Agency Research Contract (nos. 20645 and 20634); and the Global Challenges Research Fund (grant no. BB/P023223/1).

[2]These authors contributed equally to this article.

[3]Senior authors.

[4]Author for contact: ken.shirasu@riken.jp.

The author responsible for distribution of materials integral to the findings presented in this article in accordance with the policy described in the Instructions for Authors (www.plantphysiol.org) is: J. Musembi Mutuku (j.mutuku@cgiar.org).

J.M.M., S.C., S.Y., and K.Sh. participated in conception and design of the work; J.M.M., S.C., S.Y., C.H., R.N., Y.Ta., and Y.To. participated in data collection and analysis; J.M.M., S.C., S.Y., C.H., R.N., Y.To., and K.Sh. participated in data interpretation and drafting of the article; J.M.M., S.C., S.Y., T.M., T.D., T.U., K.Sa., and K.Sh. participated in critical revision of the article; all authors participated in final approval of the article to be published.

[OPEN]Articles can be viewed without a subscription.

www.plantphysiol.org/cgi/doi/10.1104/pp.18.01133

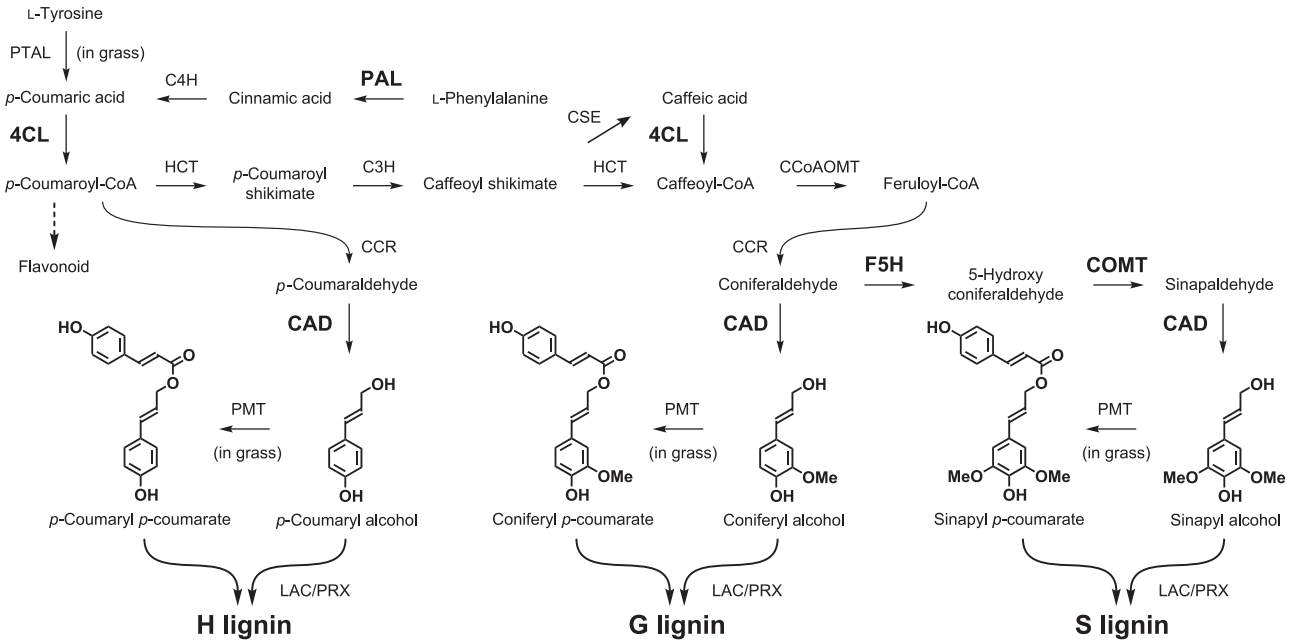


**Figure 1.** Overview of phenylpropanoid and monolignol biosynthetic pathways. The expression of the genes encoding the enzymes in bold was induced by *S. hermonthica* infection in rice roots. C4H, cinnamate 4-hydroxylase; PTAL, bifunctional Phe Tyr ammonia-lyase; 4CL, 4-coumaroyl-CoA ligase; HCT, p-hydroxycinnamoyl-CoA:shikimate p-hydroxycinnamoyl transferase; CSE, caffeoyl shikimate esterase; CCR, cinnamoyl-CoA reductase; PMT, p-coumaroyl-CoA: monolignol transferase; LAC, laccase; PRX, peroxidase.

advantages as a model system including amenability to genomic and functional analysis for molecular elucidation of resistance mechanisms (Swarbrick et al., 2008; Yoshida and Shirasu, 2009; Cui et al., 2018). It was recently shown that Nipponbare resistance to *S. hermonthica* involves a temporal coactivation of both jasmonic-acid and salicylic-acid defense pathways controlled by the transcriptional factor WRKY45 (Mutuku et al., 2015). Most of these defense responses occur as early as 1 day postinfection (dpi) and peaking at 3 dpi. Based on these findings, we reasoned that products of the phenylpropanoid pathway such as lignin, might have an important role in resistance against *S. hermonthica*.

To investigate this hypothesis, we measured changes in metabolites at the interface of host root-*S. hermonthica* haustorium at an early time point. Our nontargeted metabolome analysis suggested that lignin may play a role in *S. hermonthica* resistance. Therefore, we conducted detailed quantification and chemical analyses of the lignins produced during the resistance response against *S. hermonthica* by using a pyrolysis gas chromatography/mass spectrometry (pyrolysis-GCMS) approach. We found that lignin-derived pyrolysis products balanced with H-, G-, and S-type compounds were more abundant in Nipponbare compared to Koshihikari upon *S. hermonthica* infection. Furthermore, perturbing the balance of H-, S-, and G-type lignin polymer units by genetically modifying FERULATE 5-HYDROXYLASE (*F5H*) and *C3′H* in rice significantly increased host susceptibility to *S. hermonthica*. Together, these results demonstrate that deposition of lignin and maintenance of its structural integrity are required for resistance against *S. hermonthica*.

## RESULTS

### Changes in Metabolites of *S. hermonthica*-Infected Rice Roots at Early Infection Stages

To understand the metabolomic changes underlying *Striga* spp. resistance, we analyzed the metabolome of *S. hermonthica*-infected rice roots by liquid chromatography quadrupole time-of-flight mass spectrometry (LC-QTOF-MS) at 4 dpi. The 4-d time point was chosen because we previously found that most of attached *S. hermonthica* formed xylem–xylem connections with their host within 4 d; and that there is no apparent phenotypic difference between resistant and susceptible cultivars at this time point (Yoshida and Shirasu, 2009). The susceptible rice cultivar 'Koshihikari' and the resistant cultivar 'Nipponbare' were infected with *S. hermonthica* seeds that were pregerminated by treatment with strigol. The infected rice tissues together with *S. hermonthica* tissues were excised at 4 dpi and their metabolites were extracted. As a control, metabolites of noninfected rice roots and 4-d-old *S. hermonthica* radicles were measured. Using principal component analysis (PCA) of metabolites quantified by nontargeted profiling using both negative and positive ion modes of LC-QTOF-MS, we found that there were

significant differences among the noninfected rice control, *S. hermonthica*-infected rice roots, and *S. hermonthica* radicles. The first component (PCA1) separates metabolites in rice roots from those in *S. hermonthica* radicles, while the second component (PCA2) separates metabolites in *S. hermonthica*-infected rice roots from those in noninfected rice roots and *S. hermonthica* radicles (Fig. 2; Supplemental Fig. S1). Between the susceptible and resistant cultivars, differences were observed with or without *S. hermonthica* infections.

As the metabolites that showed different accumulation patterns between the susceptible and resistant cultivars could contribute to the resistance mechanisms, we determined the *Striga*-infected and noninfected rice metabolite structures using a rice metabolome database (Yang et al., 2014). Annotation suggested that cell wall lignin-related compounds were differentially accumulated in Nipponbare after *S. hermonthica* infection. Moreover, following *S. hermonthica* infection, phenolic acids were preferentially accumulated in Nipponbare (Supplemental Data Sets S1 and S2).

### Pyrolysis-GCMS Analysis of Cell Wall Components in *S. hermonthica*-Infected Rice Roots

To further investigate the differences in cell wall composition between *S. hermonthica*-infected resistant and susceptible rice cultivars, rice root samples were subjected to pyrolysis-GCMS analysis. *S. hermonthica* tissues were carefully removed from rice roots and only the infection sites were excised and subjected to solvent extraction followed by pyrolysis-GCMS analysis on the cell wall residues (CWRs). The pyrolysis-derived compounds were identified by comparing their mass spectra with those of 128 compounds previously identified in various cell wall pyrolysates as described in Ralph and Hatfield (1991). Among the previously assigned compounds, 73 compounds were successfully annotated. Each of the 73 identified compounds was classified into either lignin-derived compounds, carbohydrate-derived compounds or others, and lignin-derived compounds were further subclassified into H-, G-, or S-type lignin-derived compounds as described in Faix et al. (1990, 1991; Ralph and Hatfield (1991; Table 1; Supplemental Data Set S3). The area values of the total ion current spectra were determined to estimate the relative amounts of the corresponding compounds. As previously shown, pyrolysis-GCMS analyses of grasses detect large amounts of 4-vinylphenol and 4-vinylguaiacol, which seem to arise mostly from *p*-coumarates and ferulates abundant in grass cell walls, respectively (del Río et al., 2012; Moghaddam et al., 2017). Therefore, total lignin amount was estimated by summing up area values of lignin-derived compounds except for 4-vinylphenol, 4-vinylguaiacol, and the analogous 2,6-dimethoxy-4-vinylphenol (4-vinylsyringol). In addition, total carbohydrate amount was estimated by summing up the area of 18 peaks of carbohydrate-derived compounds.

Koshihikari root samples released higher levels of total lignin- and carbohydrate-derived compounds compared to those from Nipponbare roots before *S. hermonthica* infection, but there were no apparent changes in the abundance of both total lignin- and carbohydrate-derived compounds in the Koshihikari root pyrograms after infection. In contrast, Nipponbare root samples released significantly higher levels of both total lignin- and carbohydrate-derived compounds upon *S. hermonthica* infection (Fig. 3; Supplemental Data Set S3). In Nipponbare and Koshihikari rice roots, three compounds, i.e. 2,3-dihydro-5-methylfuran-2-one, 4-hydroxy-5,6-dihydro-(2*H*)-pyran-2-one, and 1,6-anhydro-$\beta$-D-glucopyranose, accounted for >70% of all carbohydrate-derived compounds, with 4-hydroxy-5,6-dihydro-(2*H*)-pyran-2-one accounting for close to half (Supplemental Data Set S3). The contents of these three compounds, all of which are supposed to be derived mainly from cellulose (Vermerris et al., 2010; Lu et al., 2016), changed upon *S. hermonthica* infection in

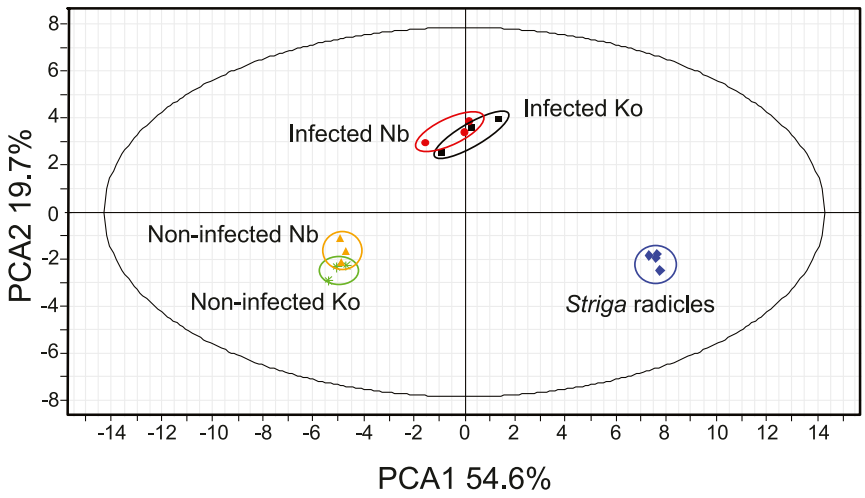


**Figure 2.** Untargeted profiling using LC-Q-TOF-MS negative ion mode of control, *S. hermonthica*-infected rice, and that of *S. hermonthica* radicles at 4 dpi of germination by strigol. Data represents three biological replications of pools of rice roots obtained as described in the "Materials and Methods." Nb, Nipponbare; Ko, Koshihikari.

**Table 1.** The H-, G-, and S-lignin-derived pyrolysis products in the control and S. hermonthica-infected rice roots of the resistant cultivar 'Nipponbare' and the susceptible cultivar 'Koshihikari'

Data are means ± SE (SE) of three biological replications. Each biological replicate contained a pool of two to five plants, from which at least four *S. hermonthica*-infected roots were obtained. In parentheses is the retention time relative to that of guaiacol. Asterisks indicate statistically significant difference between infected and control plants or between *S. hermonthica*-infected Nipponbare and Koshihikari. Student's *t* test: $*P < 0.05$, $**P < 0.01$. Nb, Nipponbare; Ko, Koshihikari.

| Compound Name (Relative Time of Guaiacol) | Nipponbare[a] | | Koshihikari[a] | | Nb FC | Ko FC | Nb/Ko FC |
|---|---|---|---|---|---|---|---|
| | Control | Infected | Control | Infected | Infected/ Control | Infected/ Control | Nb-infected/ Ko-infected |
| **H-lignin–derived** | | | | | | | |
| Phenol (0.81) | 1,270,246 ± 29,372 | 1,845,540 ± 79,604 | 1,453,507 ± 130,454 | 1,633,293 ± 33,784 | 1.5** | 1.1 | 1.1 |
| 4-Methylphenol, *p*-cresol (0.96), 3-methylphenol, m-cresol (0.97) | 400,879 ± 4,378 | 813,433 ± 57,893 | 560,418 ± 89,345 | 581,797 ± 62,150 | 2.0* | 1.0 | 1.4 |
| 4-Ethylphenol (1.11) | 34,710 ± 705 | 148,776 ± 26,295 | 96,106 ± 40,519 | 77,858 ± 43,980 | 4.3* | 0.8 | 1.9 |
| 4-Vinylphenol (1.18) | 2,494,814 ± 134,938 | 6,509,439 ± 685,101 | 4,654,667 ± 1,024,820 | 4,946,889 ± 366,924 | 2.6* | 1.1 | 1.3 |
| 4-Hydroxybenzoic acid methyl ester (1.50) | 4,044 ± 525 | 10,905 ± 1,411 | 7,578 ± 1,342 | 8,884 ± 1,336 | 2.7* | 1.2 | 1.2 |
| 4-Hydroxybenzoic acid (1.56) | 14,747 ± 1,198 | 19,176 ± 1,512 | 14,892 ± 898 | 15,763 ± 1,643 | 1.3 | 1.1 | 1.2 |
| **G-lignin–derived** | | | | | | | |
| Guaiacol (1.00) | 592,969 ± 13,684 | 904,034 ± 76,644 | 664,409 ± 83,777 | 723,499 ± 22,869 | 1.5 | 1.1 | 1.2 |
| 4-Ethylguaiacol (1.29) | 101,381 ± 3,815 | 168,154 ± 19,597 | 114,056 ± 20,107 | 102,895 ± 7,800 | 1.7 | 0.9 | 1.6* |
| 4-Vinylguaiacol (1.34) | 7,257,631 ± 120,921 | 9,211,009 ± 833,344 | 8,092,399 ± 1,503,311 | 6,358,186 ± 540,390 | 1.3 | 0.8 | 1.4* |
| Eugenol (1.40) | 32,067 ± 1,133 | 75,785 ± 7,204 | 43,470 ± 5,981 | 61,060 ± 3,910 | 2.4* | 1.4 | 1.2 |
| 4-Propylguaiacol (1.42) | 4,803 ± 204 | 9,768 ± 856 | 5,915 ± 836 | 6,758 ± 655 | 2.0** | 1.1 | 1.4* |
| Vanillin (1.44) | 380,154 ± 25,208 | 993,165 ± 117,407 | 642,882 ± 152,228 | 759,209 ± 40,750 | 2.6** | 1.2 | 1.3 |
| Cis-isoeugenol (1.47) | 14,470 ± 127 | 22,511 ± 2,626 | 16,505 ± 2,887 | 15,245 ± 1,375 | 1.6 | 0.9 | 1.5 |
| Homovanillin (1.52) | 13,794 ± 1,091 | 20,999 ± 2,071 | 15,641 ± 2,279 | 17,369 ± 2,400 | 1.5* | 1.1 | 1.2 |
| Transisoeugenol (1.52) | 115,861 ± 2,535 | 321,691 ± 32,588 | 174,448 ± 24,417 | 254,758 ± 19,272 | 2.8* | 1.5 | 1.3 |
| Acetovanillone (1.56) | 18,189 ± 10,078 | 16,126 ± 610 | 10,787 ± 1,116 | 14,457 ± 1,762 | 0.9 | 1.3 | 1.1 |
| 1-(4-Hydroxy-3-methoxyphenyl)propyne (1.56) | 18,660 ± 1,038 | 48,196 ± 3,634 | 26,111 ± 3,900 | 45,947 ± 2,037 | 2.6** | 1.8* | 1.0 |
| 1-(4-Hydroxy-3-methoxyphenyl)allene (1.57) | 15,933 ± 811 | 43,269 ± 3,111 | 24,907 ± 4,740 | 41,764 ± 3,009 | 2.7** | 1.7* | 1.0 |
| Vanillic acid methyl ester (1.58) | 2,136 ± 137 | 3,558 ± 380 | 1,725 ± 286 | 2,952 ± 424 | 1.7* | 1.7 | 1.2 |
| Guaiacylacetone (1.61) | 9,211 ± 191 | 24,013 ± 2,395 | 11,469 ± 2,382 | 17,706 ± 1,490 | 2.6* | 1.5 | 1.4 |
| Vanillic acid (1.63) | 1,560 ± 126 | 2,449 ± 318 | 2,002 ± 138 | 1,677 ± 75 | 1.6 | 0.8 | 1.5 |
| Propiovanillone (1.66) | 2,197 ± 228 | 7,184 ± 678 | 4,330 ± 1,176 | 5,196 ± 1,063 | 3.3** | 1.2 | 1.4 |
| Guaiacyl vinyl ketone (1.67) | 2,669 ± 207 | 6,734 ± 430 | 4,354 ± 666 | 5,467 ± 427 | 2.5** | 1.3 | 1.2 |
| Cis-coniferyl alcohol (1.76) | 475 ± 77 | 7,225 ± 1,146 | 3,530 ± 890 | 5,594 ± 1,282 | 15.2* | 1.6 | 1.3 |
| Transconiferaldehyde (1.84) | 6,849 ± 914 | 39,102 ± 4,576 | 18,223 ± 3,318 | 35,559 ± 3,212 | 5.7* | 2.0* | 1.1 |
| Transconiferyl alcohol (1.85) | 2,775 ± 231 | 29,533 ± 5,410 | 14,193 ± 3,092 | 27,849 ± 5,680 | 10.6* | 2.0 | 1.1 |
| **S-lignin–derived** | | | | | | | |
| 2,6-Dimethpxyphenol (1.38) | 247,775 ± 2,869 | 531,627 ± 60,415 | 339,686 ± 78,624 | 379,911 ± 25,686 | 2.1* | 1.1 | 1.4 |
| 2,6-Dimethoxy-4-methylphenol (1.50) | 165,457 ± 5,111 | 368,493 ± 48,984 | 233,368 ± 48,881 | 227,911 ± 216,23 | 2.2 | 1.0 | 1.6 |
| 4-Ethyl-2,6-dimethoxyphenol (1.60) | 14,251 ± 285 | 28,021 ± 3,799 | 18,352 ± 2,380 | 16,972 ± 1,210 | 2.0 | 0.9 | 1.7 |
| 2,6-Dimethoxy-4-vinylphenol (1.65) | 238,975 ± 3,360 | 523,463 ± 64,666 | 320,357 ± 63,586 | 375,457 ± 23,647 | 2.2* | 1.2 | 1.4 |
| 4-Allyl-2,6-dimethoxyphenol (1.69) | 68,774 ± 1,284 | 151,548 ± 18,591 | 97,133 ± 19,695 | 104,069 ± 9,975 | 2.2* | 1.1 | 1.5 |
| 2,6-Dimethoxy-4-propylphenol (1.71) | 4,281 ± 250 | 9,076 ± 1,146 | 5,779 ± 873 | 5,561 ± 253 | 2.1* | 1.0 | 1.6 |
| Syringaldehyde (1.75) | 52,870 ± 2,022 | 161,372 ± 22,785 | 93,299 ± 23,055 | 114,677 ± 10,045 | 3.1* | 1.2 | 1.4 |
| Cis-2,6-dimethoxy-4-propenylphenol (1.75) | 50,618 ± 486 | 127,789 ± 11,974 | 78,130 ± 12,948 | 92,095 ± 8,456 | 2.5* | 1.2 | 1.4 |
| Homosyringaldehyde (1.80) | 741 ± 126 | 111 ± 61 | 559 ± 282 | 457 ± 324 | 0.2* | 0.8 | 0.2 |

(*Table continues on following page.*)

**Table 1.** (*Continued from previous page.*)

| Compound Name (Relative Time of Guaiacol) | Nipponbare[a] | | Koshihikari[a] | | Nb FC Infected/ Control | Ko FC Infected/ Control | Nb/Ko FC Nb-infected/ Ko-infected |
|---|---|---|---|---|---|---|---|
| | Control | Infected | Control | Infected | | | |
| 1-(3,5-Dimethoxy-4-hydroxyphenyl) propyne (1.80) | 29,974 ± 811 | 69,727 ± 7,295 | 48,014 ± 8,540 | 62,367 ± 3,977 | 2.3* | 1.3 | 1.1 |
| Trans-2,6-dimethoxy-4-propenylphenol (1.81) | 290,064 ± 5,771 | 782,051 ± 78,985 | 436,701 ± 85,610 | 546,315 ± 49,671 | 2.7* | 1.3 | 1.4 |
| Acetosyringone (1.83) | 17,093 ± 182 | 48,955 ± 6,247 | 25,882 ± 5,363 | 36,040 ± 2,387 | 2.9* | 1.4 | 1.4 |
| Syringylacetone (1.87) | 1,045 ± 150 | 30,919 ± 3,634 | 16,874 ± 4,034 | 22,125 ± 2,095 | 2.8* | 1.3 | 1.4 |
| Syringic acid methyl ester (1.87) | 1,811 ± 167 | 2,754 ± 303 | 1,976 ± 185 | 2,939 ± 293 | 1.5 | 1.5 | 0.9 |
| Syringic acid (1.87) | 655 ± 265 | 329 ± 165 | 582 ± 301 | 996 ± 751 | 0.5 | 1.7 | 0.3 |
| 3-(3,5-Dimethoxy-4-hydroxyphenyl)-3-oxopropanal (1.93) | 2,690 ± 229 | 6,372 ± 780 | 4,216 ± 1,125 | 3,505 ± 490 | 2.4* | 0.8 | 1.8* |
| Propiosyringone (1.93) | 6,243 ± 367 | 17,788 ± 2,135 | 9,368 ± 865 | 12,439 ± 1,007 | 2.8* | 1.3 | 1.4 |
| Syringyl vinyl ketone (1.93) | 2,245 ± 406 | 4,711 ± 1,398 | 4,260 ± 693 | 3,165 ± 291 | 2.1 | 0.7 | 1.5 |
| Dihydrosinapyl alcohol (2.00) | 1,621 ± 136 | 4,224 ± 1,359 | 3,199 ± 602 | 6,485 ± 442 | 2.6 | 2.0* | 0.7 |
| Cis-sinapyl alcohol (2.02) | 365 ± 123 | 3,128 ± 434 | 1,452 ± 151 | 2,546 ± 254 | 8.6** | 1.8* | 1.2 |
| Transsinapaldehyde (2.09) | 1,277 ± 60 | 2,826 ± 324 | 1,559 ± 488 | 1,662 ± 179 | 2.2* | 1.1 | 1.7* |
| Transsinapyl alcohol (2.09) | 1,384 ± 160 | 9,469 ± 1,511 | 5,365 ± 597 | 8,068 ± 992 | 6.8* | 1.5 | 1.2 |
| **Other lignin-derived compounds** | | | | | | | |
| 4-Methoxytoluene (0.90)_3-methoxytoluene (0.90) | 13,947 ± 342 | 24,991 ± 1,723 | 15,499 ± 2,265 | 20,736 ± 835 | 1.8* | 1.3 | 1.2 |
| 2-Methylphenol, o-cresol (0.93) | 58,793 ± 1,520 | 108,422 ± 7,842 | 71,604 ± 9,795 | 81,236 ± 5,608 | 1.8* | 1.1 | 1.3 |
| 2,6-Dimethylphenol (1.03) | 3,932 ± 1,004 | 6,258 ± 3,337 | 3,965 ± 1,394 | 6,299 ± 1,497 | 1.6 | 1.6 | 1.0 |
| 2,4-Dimethylphenol (1.08) | 23,350 ± 296 | 56,546 ± 4,615 | 33,325 ± 6,055 | 36,353 ± 4,316 | 2.4* | 1.1 | 1.6 |
| Catechol (1.14) | 2,020 ± 682 | 240,049 ± 48,230 | 169,641 ± 54,198 | 205,743 ± 34,391 | 118.8* | 1.2 | 1.2 |
| 3-Methoxycatechol (1.26) | 36,340 ± 4,058 | 156,635 ± 24,403 | 95,841 ± 25,186 | 120,629 ± 12,172 | 4.3* | 1.3 | 1.3 |
| 4-Methoxycatechol (1.27) | 3,649 ± 1,829 | 65,816 ± 13,206 | 23,198 ± 10,183 | 31,514 ± 7,688 | 18.0* | 1.4 | 2.1 |

[a]Peak area values of the GC-MS total ion-current chromatograms of the pyrolysates.

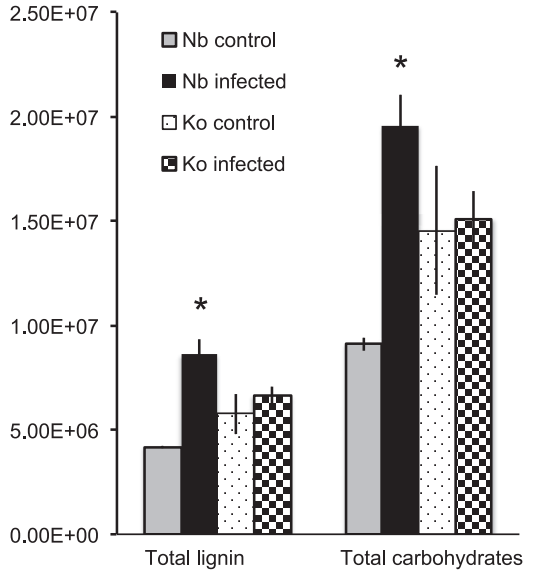


**Figure 3.** Lignin and carbohydrate contents in rice roots under control conditions or infected with *S. hermonthica* at 4 dpi as estimated by pyrolysis-GCMS. Total lignin amount was calculated by summing up area values in each pyrogram of lignin-derived compounds except for 4-vinylphenol, 4-vinyl-guaiacol, and the analogous 2,6-dimethoxy-4-vinylphenol (4-vinylsyringol), whereas total carbohydrate amount was determined by summing up the area of 18 peaks derived from carbohydrates as listed in Supplemental Data Set S3. Values represent mean ± SE. Asterisks (*) indicate statistically significant differences (Student's *t* test, $P < 0.05$) between control and *S. hermonthica*-infected plants. Nb, Nipponbare; Ko, Koshihikari.

Nipponbare but not in Koshihikari (Supplemental Data Set S3).

Many of the lignin-derived compounds identified in the pyrograms of Nipponbare roots increased upon *S. hermonthica* infection, whereas, only a few significantly increased in the pyrograms of Koshihikari roots (Table 1). Among the 20 G-lignin-derived compounds detected in this study, only acetovanillone was released at lower levels from *S. hermonthica*-infected Nipponbare roots compared to the control roots with a fold change (*FC*) = 0.9. The levels of all other compounds were higher in *S. hermonthica*-infected Nipponbare root pyrograms compared to those in the control non-infected root pyrograms, with cis-coniferyl alcohol (*FC* = 15.2) and transconiferyl alcohol (*FC* = 10.6) having the largest change (Table 1). Most of the S-lignin–derived compounds also increased after *Striga* infection; 16 out of 22 compounds showed significantly higher amounts in infected samples compared to the non-infected control in Nipponbare, while only 2 of 22 compounds showed significant changes in the *Striga*-susceptible cultivar Koshihikari. The products that increased the most were cis- and transsinapyl alcohol (*FC* = 8.6 and 6.8, respectively), which represent core lignin products arising from pyrolysis of the S-type lignin polymers (Table 1; Supplemental Data Set S3). The levels of the H-lignin-derived compounds (i.e. phenol, the sum of 4-methylphenol, *p*-cresol, 3-methylphenol and m-cresol, 4-ethylphenol, and 4-hydroxybenzoic acid methyl ester) were also significantly higher in Nipponbare (Student's *t* test, $P < 0.05$) after *S. hermonthica* infection (Table 1). In addition, catechol, 3-methoxycatechol, and 4-methoxycatechol largely increased by 119-fold, 4-fold, and 18-fold, respectively, in Nipponbare (Table 1). In contrast, such changes were not apparent in Koshihikari (Table 1; Supplemental Data Set S3). Taken together, total amounts of pyrolysis products from each lignin type (i.e. H, G, S, and others) show significant changes in rice roots upon *S. hermonthica* infection in the resistant cultivar Nipponbare (Table 2). The proportional changes in lignin composition were estimated by the ratio between each one of the product types (H, G, and S) and the sum of all the product types identified in this study; it should be noted that H-units could be substantially overestimated because some of the H-lignin marker products (such as phenol) can be released not only from H-lignins but also from cell wall proteins, especially from their Tyr residues, upon pyrolysis (Ralph and Hatfield, 1991; Li et al., 2012). The proportions of H- and G-lignin–derived pyrolysis products did not show significant difference, whereas S-lignin–derived pyrolysis products increased significantly in Nipponbare (Student's *t* test, $P < 0.05$; Table 2; Supplemental Data Set S3). Accordingly, the S/G ratio also showed significant changes in Nipponbare after *Striga*-infection but not in Koshihikari although the proportion of G-lignin derived products slightly increased in Koshihikari (Table 2).

### Expression of Lignin Biosynthesis Genes Increases upon *S. hermonthica* Infection

To investigate whether the lignin-related metabolite changes are under transcriptional regulation, we examined the expression of genes encoding major enzymes in the lignin biosynthesis pathway (Fig. 1), i.e. Phe ammonia lyase1 (*OsPAL1*; Cass et al., 2015), 4-coumaroyl-CoA ligase3 (*Os4CL3*; Gui et al., 2011), F5H1 (*OsF5H1*; Takeda et al., 2017), cinnamyl alcohol dehydrogenase2 (*OsCAD2*; Zhang et al., 2006), and caffeic acid o-methyltransferase1 (*OsCOMT1*; Koshiba et al., 2013) by quantitative reverse transcription PCR (RT-qPCR; Supplemental Table S1). The *OsPAL1* expression was induced at 1 dpi and increased 6-fold to reach the maximum expression levels at 3 dpi in Nipponbare (Fig. 4A). The expression of *Os4CL3* increased specifically in Nipponbare from 1 dpi reaching 5-fold compared to the noninfected control plants at 3 dpi (Fig. 4B) as was the case with *OsF5H1* expression, which was induced at 1 dpi and increased to more than 2-fold at 3 dpi (Fig. 4C). The expression of *OsCAD2* was induced with maximum expression levels at 3 dpi (Fig. 4D). *OsCOMT1* expression was induced in *S. hermonthica*-infected roots of Nipponbare at 3 dpi before reducing to the basal levels at 7 dpi. In *S. hermonthica*-infected

**Table 2.** Pyrolysis-GCMS-derived rough estimation of lignin composition in the root infection sites of the resistant cultivar 'Nipponbare' and the susceptible cultivar 'Koshihikari' in control and S. hermonthica-infected plants

Data are calculated by sum of integral peaks from each lignin-type product listed in Table 1 (excluding 4-vinylphenol, 4-phenolguaiacol, and 2,6-dimethoxyl-4-vinylphenol, which can be derived from cell-wall–bound cinnamates). Means ± SE (SE) of three biological replications (each of which contained a pool of two to five plants) are shown. Values in parentheses are percentage to the total of H + G + S products. H-products may include phenols originated from cell wall proteins (see text). Student's *t* test: $*P < 0.05$, $**P < 0.01$; comparing control and *Striga*-infected plants.

| Lignin Polymer Unit | Nipponbare | | Koshihikari | |
|---|---|---|---|---|
| | Control | *Striga*-infected | Control | *Striga*-infected |
| H | 1,724,625 ± 33,128 | 2,837,829 ± 137,589** | 2,132,501 ± 260,861 | 2,317,594 ± 139,525 |
| (%) | (42.8 ± 0.4) | (36.0 ± 1.9) | (40.4 ± 1.9) | (37.9 ± 0.2) |
| G | 1,336,152 ± 21,558 | 2,743,496 ± 275,218* | 1,798,957 ± 312,049 | 144,959 ± 117,937 |
| (%) | (33.1 ± 0.3) | (34.4 ± 0.7) | (33.4 ± 0.5) | (35.1 ± 0.4)* |
| S | 971,234 ± 8,196 | 2,361,291 ± 270,431* | 1,425,754 ± 293,902 | 1,650,304 ± 137,044 |
| (%) | (24.1 ± 0.4) | (29.6 ± 1.2)* | (26.2 ± 1.4) | (26.9 ± 0.5) |
| S/G | 0.73 ± 0.02 | 0.86 ± 0.02** | 0.78 ± 0.03 | 0.77 ± 0.02 |

roots of Koshihikari, its expression appeared to be suppressed compared to the healthy control plants (Fig. 4E). These results suggest that genes in the lignin biosynthesis pathway are up-regulated at an early time point after *S. hermonthica* infection, especially in the resistant cultivar. This is consistent with the findings of the metabolite and cell wall analyses, which showed that lignin and its associated phenolics accumulate in the resistant cultivar as early as 4 dpi.

### Lignin Is Deposited at the Interface between the Host and *S. hermonthica*

To analyze the localization of lignin accumulation upon *S. hermonthica* infection, lignin staining was performed on the roots of Koshihikari and Nipponbare 4 d after *S. hermonthica* infection. The phloroglucinol-HCl staining, which primarily reacts with the cinnamaldehyde end-units in lignin polymers, revealed the presence of lignin inside the vasculature of intact or *S. hermonthica*-infected rice roots of both cultivars (Fig. 5). The innermost cell layers (which include cells around the metaxylem) in both Nipponbare and Koshihikari showed strong staining, whereas the endodermal cells were mostly unstained (Fig. 5). However, a clear distinction between the two rice cultivars was the observation that a stronger staining intensity was often detected at the *S. hermonthica* invasion site in Nipponbare (Fig. 5). Such lignin staining was restricted to the apoplastic region of a few cells surrounding *S. hermonthica* haustoria (Fig. 5). This strongly supports our contention that resistance against *S. hermonthica* correlates with the local accumulation of lignin at the site of infection.

### The Composition of Tissue Lignin Determines Host Resistance against *S. hermonthica*

Evidence for the role of soluble phenolics, lignin, and lignin composition in plant defense has been obtained from the analysis of transgenic plants and mutants with varying lignin contents and composition (Bhuiyan et al., 2009; Funnell-Harris et al., 2010; Maury et al., 2010; Gallego-Giraldo et al., 2011). To determine the role of lignin in rice resistance against *S. hermonthica*, we used transgenic Nipponbare in which *C3′H* is down-regulated by RNA interference (*OsC3′H*-kd; Takeda et al., 2018). As *C3′H* provides entry into the main lignin biosynthetic pathway leading to the formation of G- and S-type monolignols but not H-type monolignol (Fig. 1), the disruption of *C3′H* in various plants results in increased incorporation of H-units at the expense of the normally dominant G- and/or S-units in lignins produced in major vegetative tissues (Abdulrazzak et al., 2006; Ralph et al., 2006; Bonawitz et al., 2014; Takeda et al., 2018). Consistently, our nuclear magnetic resonance (NMR) and thioacidolysis analyses on the roots of *OsC3′H*-kd showed that the relative proportion of H-units in lignin increased 6-fold and was accompanied by a 3-fold reduction of G-units compared to the wild-type plants. No significant change was observed in S-units (Supplemental Fig. S2, A and B). Also, in *OsC3′H*-kd roots, a reduction in total lignin content as determined by the thioglycolic lignin assay was observed (Supplemental Fig. S2C), which is consistent with findings reported in Arabidopsis where disruption of *C3′H* reduces the amount of lignin in root cell walls (Abdulrazzak et al., 2006; Takeda et al., 2018). In contrast to the case in stem cell walls (Takeda et al., 2018), root cell walls from both *OsC3′H*-kd and wild-type rice did not have detectable levels of tricin, a flavonoid, which is integrated as a major component of grass lignins (Supplemental Fig. S2A; Lan et al., 2015). We infected the roots of *OsC3′H*-kd transgenic and wild-type plants with germinated *S. hermonthica* seedlings and quantified the *S. hermonthica* survival rate by measuring the number of *S. hermonthica* plants that produced at least six leaves (Fig. 6). At 50 d after infection, ~3% of *S. hermonthica* survived on the wild-type plants. In *OsC3′H*-kd plants infected with *S. hermonthica*, there was a 4-fold increase in survival rate (Fig. 6, A and C),

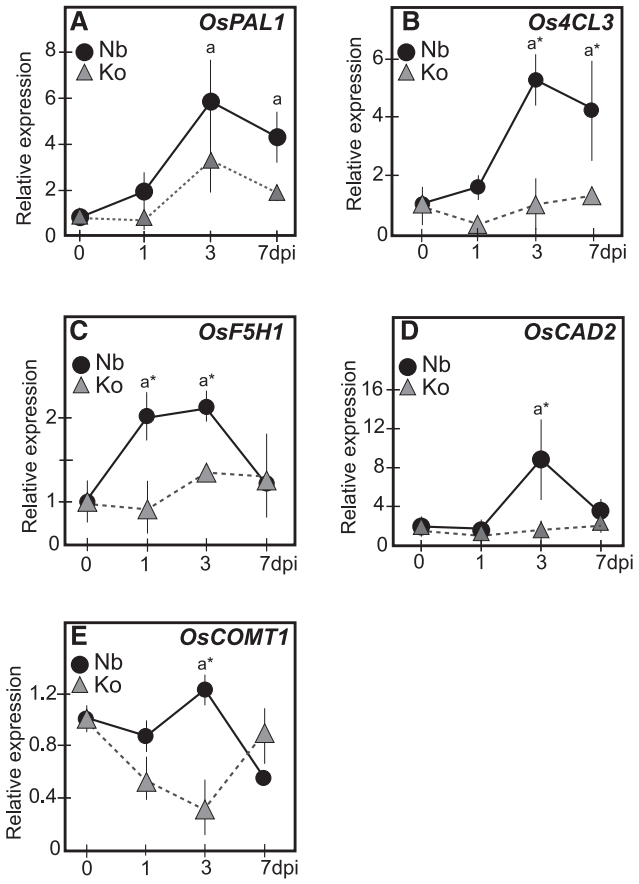


**Figure 4.** *Striga* infection induces the expression of phenylpropanoid pathway genes. Expression of *OsPAL1* (A), *Os4CL3* (B), *OsF5H1* (C), Os*CAD2* (D), and *OsCOMT* (E) in the *Striga*-infected roots of Nipponbare (closed circles) and Koshihikari (closed triangles) at 0, 1, 3, and 7 dpi. Three biological and three technical replicates each containing a pool of roots from at least five plants were analyzed. Values represent mean ± SE. Gene expression was normalized using *Oscyclophilin*. Letters indicate statistically significant differences (Student's *t* test, $P < 0.05$) from 0 dpi. Asterisks (*) indicate statistically significant differences (Student's *t* test, $P < 0.05$) among rice cultivars. Nb, Nipponbare; Ko, Koshihikari.

showing enhanced susceptibility of *OsC3′H*-kd plants toward *S. hermonthica*.

We also performed infection experiments using transgenic Nipponbare carrying small interference RNA targeting rice *F5H* (*OsF5H*-kd) or the modified rice *polyubiquitin1* promoter-driven *F5H* coding sequence (*OsF5H*-OX; Takeda et al., 2017; Cui et al., 2018); *F5H* is one of the key enzymes mediating the synthesis of S-lignin (Fig. 1). *OsF5H*-kd roots accumulate less S- and more G-lignin polymers (S/G ratio, 4:6, based on NMR), whereas *OsF5H*-OX roots accumulates more S- and fewer G-lignin polymers (S/G ratio, 7:3, based on NMR) compared to the wild-type plants (S/G ratio, 5:5, based on NMR); no differences were found in either total lignin or H-lignin between the transgenics and the wild-type plants (Cui et al., 2018). After one month, infection to either *OsF5H*-kd or *OsF5H*-OX plants increased *S. hermonthica* survival rates 2-fold compared to those infecting the wild-type plants (Fig. 6, B and D). *S. hermonthica* on transgenic plants showed a growth rate similar to those on the wild-type plants as indicated by the number of leaves (Fig. 6, C and D). Collectively, these results demonstrate that disruption of lignin composition balanced with H-, G-, and S-units increases host susceptibility to *S. hermonthica* infection. Thus, the maintenance of the structural integrity of tissue lignin is important in providing an appropriate defensive layer against the parasite.

## DISCUSSION

The rice cultivar Nipponbare shows resistance to *S. hermonthica* parasitism, but the underlying mechanisms for its resistance are unknown. In this study, we investigated the metabolomic differences between susceptible and resistant cultivars using nontargeted liquid chromatography-mass spectrometry and pyrolysis-GCMS analyses. We found that resistance against *S. hermonthica* is associated with an increase in lignin deposition at the site of interaction. Consistently, the phenylpropanoid pathway genes in Nipponbare are induced at earlier time points, starting at 1 dpi with a peak at 3 dpi, before returning to the basal levels by 7 dpi (Fig. 4). Because lignification is not only caused by infection (Verhage et al., 2010) but also by wounding (Becerra-Moreno et al., 2015), it is possible that the early induction of the phenylpropanoid pathway characterized by induction of metabolic pathway genes in Nipponbare is due to the damage caused by *S. hermonthica*, as host cell wall degradation precedes *S. hermonthica* penetration (Yoshida and Shirasu, 2009). The expression of some of the phenylpropanoid pathway genes reduces to basal levels by 7 dpi, perhaps because the wounding site is sealed by this time point after lignin deposition.

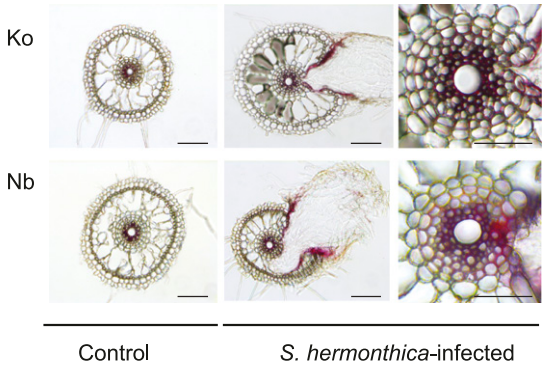


**Figure 5.** Lignin is deposited at the interface between the host and *S. hermonthica*. The localization of lignin detected by phloroglucinol-HCl staining showing the presence of lignin inside the root cells of control and *S. hermonthica*-infected rice roots of both Nipponbare and Koshihikari. (Left and center) Bars = 100 μm; (right) bars = 50 μm. Nb, Nipponbare; Ko, Koshihikari.

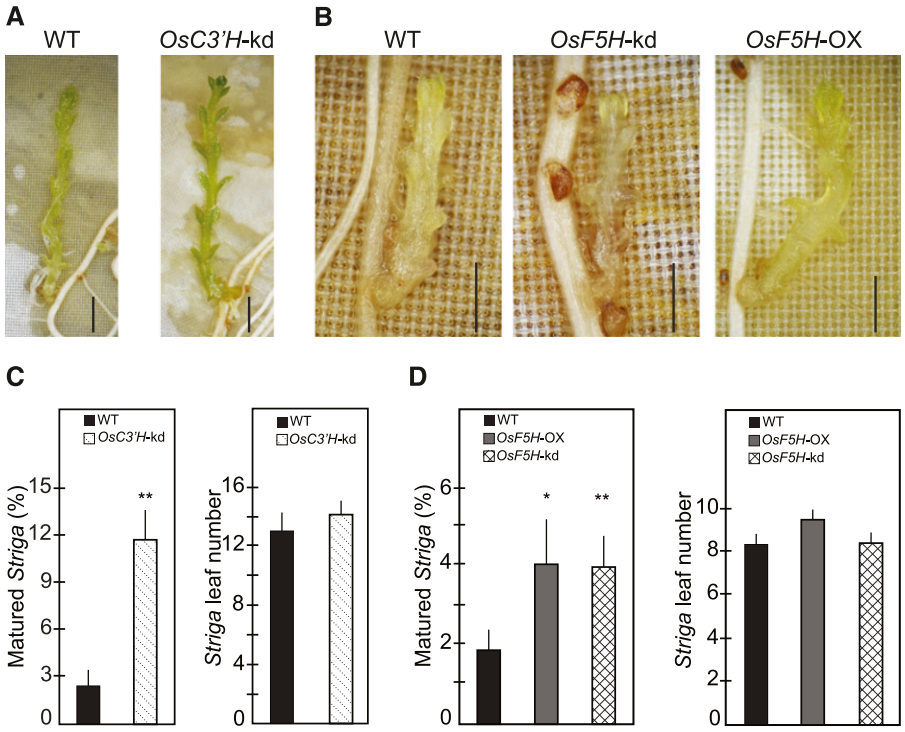


**Figure 6.** The composition of tissue lignin determines host resistance. A and B, *S. hermonthica* infection phenotypes of wild-type Nipponbare. *OsC3′H*-kd, *OsF5H*-kd, and *OsF5H*-OX rice plants. C and D, Effects of inhibiting *OsC3′H* and *OsF5H* or overexpression of *OsF5H* on host resistance against *S. hermonthica*. Values represent means ± SE of the percentage of matured *S. hermonthica* and their leaf numbers determined as described in "Materials and Methods." Data are from two independent experiments containing 13 wild-type and 14 mutant plants. Observations were made at 50 dpi. *Statistically significant difference (Student's *t* test, $P < 0.05$) from wild type. **Statistically significant difference (Student's *t* test, $P < 0.01$) from wild type. Bars = 2 mm. WT, wild type.

Although there is evidence suggesting that lignin produced during pathogen infection plays an important role in resistance against various pathogens (Caño-Delgado et al., 2003; Gunnaiah et al., 2012; Mutuku and Nose, 2012), little is known about its involvement in monocot roots responding to infection by *Striga* spp. Previous studies showed that Nipponbare induces physical defense responses that impede *S. hermonthica* ingression at the endodermis layer (Gurney et al., 2006; Yoshida and Shirasu, 2009). Quantification of cell wall constituents allowed us to determine the components that possibly cause the physical barrier against *S. hermonthica* infection. Indeed, the staining experiments showed that deposition of lignin around the site of the host-*S. hermonthica* interaction coincides with resistance (Fig. 5). This increase in lignification around the site of infection was corroborated by the pyrolysis-GCMS analysis that showed a concomitant increase in many of the lignin-derived pyrolysis products, especially in Nipponbare (Table 1; Fig. 3; Supplemental Data Set S3). The estimation of lignin composition by pyrolysis-GCMS suggested that there was an increase in the proportions of S-lignin–derived products, but not H- and G-lignin–derived products (Table 2). S-lignins and related soluble metabolites are known to contribute to resistance against fungal pathogen, as shown in the Arabidopsis *f5h* mutant whose increased susceptibility to *Verticillium longisporum* is linked to its accumulation of more G-lignins at the expense of S-lignins (König et al., 2014). In addition, the *S. hermonthica*-infected roots of Nipponbare released higher levels of carbohydrate-derived compounds compared to those of control plants and infected roots of Koshihikari (Fig. 3). As cell walls are rich in cellulosic and hemicellulosic glucans (Pattathil et al., 2015), it was unsurprising that the contents of glucan-derived compounds, such as 2,3-dihydro-5-methylfuran-2-one, 4-hydroxy-5,6-dihydro-(2*H*)-pyran-2-one, and 1,6-anhydro-*β*-D-glucopyranose, increased upon infection. As *Striga* spp. infection includes degradation of host cell walls, it is likely that the incorporation of certain polysaccharides into the cell wall complex may limit the ability of *Striga* spp. to penetrate host root tissues after attachment.

The *OsC3′H*-kd plants (Takeda et al., 2018) showed increased susceptibility when exposed to pregerminated *S. hermonthica* (Fig. 6). This suggests that accumulation of H-lignin at the expense of G lignin makes rice more susceptible to *S. hermonthica* perhaps due to a compromised ability to withstand attack by the hydrolytic enzymes of *S. hermonthica*. As *OsC3′H*-kd plants also have lower levels of total lignin contents (Supplemental Fig. S2), however, we cannot rule out the possibility that the enhanced susceptibility to *S. hermonthica* in *OsC3′H*-kd plants is also due to the impaired function of the lignin biosynthesis pathway. Modulation of *F5H* activity did not change total lignin levels in rice roots (Cui et al., 2018). However, deposition of cell walls rich in S-lignin, as is the case with *OsF5H*-OX plants (Takeda et al., 2017), resulted in increased susceptibility to *S. hermonthica* parasitism (Fig. 6). Additionally, inhibiting accumulation of lignin rich in S-units, as is the case with *OsF5H*-kd plants, also resulted in increased susceptibility to *S. hermonthica* parasitism (Fig. 6).

The susceptibility of *C3′H*- and *F5H*-modulated plants to *S. hermonthica* parasitism may result from a

redirection of carbon flux in rice roots, although the manner in which this redirection affects susceptibility to *S. hermonthica* parasitism is yet to be elucidated. The modulation of lignin biosynthetic genes may affect carbon flux between the monolignol/cinnamate and flavonoid pathways. In particular, plants disrupted in the early steps in the monolignol/cinnamate pathway occasionally display overaccumulation of flavonoids along with depletions in the amount of lignins and/or their associated metabolites (Hoffmann et al., 2004; Abdulrazzak et al., 2006; Vanholme et al., 2012; Takeda et al., 2018). Indeed, Takeda et al. (2018) demonstrated that *OsC3′H*-kd rice produced altered lignins enriched with the flavonoid tricin units in culm tissues. Such carbon flux redirections from the monolignol/cinnamate pathway to the flavonoid pathway, however, may not be prominent in the rice root tissues tested in this study, because flavonoid contents are typically very low in roots compared to other aerial parts in rice (Dong et al., 2014). In fact, our NMR failed to detect lignin-integrated tricin units in root cell walls from both *OsC3′H*-kd and wild-type rice (Supplemental Fig. S2). Meanwhile, we conjecture that changes in the phenylpropanoid pathway resulting in altered cell wall biochemistry affects the degree of incorporation of lignin and other cell wall components. This might limit the ability of cell walls to recognize or resist the spread of pathogen-derived factors for the establishment of parasitism. For example, it was recently shown that in the interaction between *Phtheirospermum japonicum* and the susceptible host Arabidopsis, the movement of a parasite-derived hormone modified both host root morphology and fitness to allow for enhanced efficiency of transfer of water and nutrients from the host (Spallek et al., 2017). Taken together, our data suggest that susceptibility to *Striga* spp. parasitism is enhanced when plants do not elevate the accumulation of lignin, as is the case in Koshihikari and *OsC3′H*-kd plants (Figs. 3 and 5; Supplemental Fig. S2) when total lignin levels are similar to those of wild-type Nipponbare plants but *F5H* activity is modulated (Fig. 6; Cui et al., 2018), and when lignin composition is altered in favor of the accumulation of any of the three lignin units, H, S and G, in rice roots, as is in the case in *OsC3′H*-kd, *OsF5H*-kd, and *OsF5H*-OX plants tested in this study (Fig. 6).

Our recent study showed that lignin monomers and lignin degradation products, particularly G- and S-type phenolics bearing at least one methoxyl group on their aromatic rings, serve as haustorium-inducing factors for *S. hermonthica*. Perturbation of either G- or S-lignin units in rice and Arabidopsis induces less haustorial formation at the early infection stage (Cui et al., 2018). Therefore, targeting lignin composition, i.e. by genetically inhibiting the biosynthesis of G- and S-lignins, may provide the host a layer of preattachment resistance against *S. hermonthica*. However, our current findings with genetic and molecular analyses reveal an anticipated role of the integrity of the lignin structure for host postattachment resistance to *S. hermonthica* infection, and thus pose a new challenge for targeting the host cell wall against *Striga* spp. infection.

## MATERIALS AND METHODS

### Plant Materials and Growth Conditions

Plant materials used and growth conditions were as reported in Yoshida and Shirasu (2009) with a few changes. Briefly, *Striga hermonthica* seeds collected from a field in Kano Nigeria were a kind gift by Dr. Alpha Kamaro of the International Institute of Tropical Agriculture Kano. The wild-type rice seeds (*Oryza sativa japonica*, 'Nipponbare', and 'Koshihikari') were obtained from the National Institute of Biological Sciences (Tsukuba, Japan). Nipponbare *OsC3′H*-kd, *OsF5H*-kd, and *OsF5H*-ox transgenic plants were derived from Takeda et al. (2017, 2018. Rice seeds were dehusked and sterilized with 10% (v/v) commercial bleach solution for 15 min and washed thoroughly with distilled water. Surface-sterilized rice plants were grown on a petri dish with sterilized water and then placed vertically in the rhizotron system to promote root extension for infection at 16-h light/8-h dark cycles at 26°C for 1 week as described in Mutuku et al. (2015). Briefly, one-week-old rice seedlings were transferred to the rhizotrons (10-cm × 14-cm–square petri dish, filled with rockwool [Nichiasu] onto which a 100-$\mu$m nylon mesh was placed) and fertilized with one-half-strength Murashige & Skoog medium. The rhizotrons were then kept in growth chambers at a temperature cycle of 28°C/23°C for a 16-h-light/8-h-dark cycle. After two weeks, the growing rice plants were inoculated with pregerminated *S. hermonthica* seeds. The *S. hermonthica* seeds were preconditioned by treating them with 10 nM of strigol (a gift from Dr. K. Mori; Hirayama and Mori, 1999) for 2–6 h to synchronously induce germination and were carefully placed next to roots of each rice plant. The rhizotrons containing inoculated plants were placed back into the growth chambers and incubated under the same conditions until sampling.

### Quantification of Postattachment Resistance

After 3 d of infection, *S. hermonthica* seedlings that formed haustoria were counted under stereomicroscopy (Stemi 200-C; Zeiss) as the total number of *S. hermonthica*. *S. hermonthica* plants producing at least six leaves were determined under stereomicroscopy (Stemi 200-C; Zeiss) and marked as matured *S. hermonthica* and used for quantification assays. The rate of successful *S. hermonthica* infection was determined as a percentage of matured *S. hermonthica* against the total number of *S. hermonthica* seedlings to avoid overestimation that was noticed to occur when using the total number of *S. hermonthica* seeds instead of the total number of attached *S. hermonthica* seeds (Mutuku et al., 2015).

### Sampling

Sampling was done at 4 dpi. Rice roots were cut in a manner to collect only the host-*S. hermonthica* interaction sites, and were immediately transferred into chilled 2 mL tubes with a steel top (Bristol-Myers Squibb) and frozen in liquid N before storage at −80°C. These samples were processed for use in liquid chromatography-mass spectrometry or pyrolysis-GCMS. Each biological replicate contained a pool of two to five plants, from which at least four *S. hermonthica*-infected roots were obtained.

### Rice Root Staining for Lignin

Growth conditions of rice and germination of *S. hermonthica* seeds were described in Cui et al. (2016), Mutuku et al. (2015), and Yoshida and Shirasu (2009). All the processes were performed at 25°C under an 18-h/6-h light/dark cycle. Surface-sterilized rice plants were germinated in water for 1 week and transferred to a rhizotron followed by roots growing vertically for 1 week before infection. Germinated *S. hermonthica* seedlings after 24 h of strigol treatment (Hirayama and Mori, 1999) were placed on the surface of the rice roots 1–4 cm above the root tips. At 4 dpi, root segments with attached haustoria were excised, imbedded in 7% (w/v) agar, and sectioned by a vibratome (HM 650 V; MICROM). Sections with 40-$\mu$m thickness were stained in 1% (w/v) phloroglucinol solution containing 18% (v/v) HCl for 5 min and observed under a light microscope (DMI 3000 B; Leica).

## Metabolites Extraction Method

The samples were mixed with 100 $\mu$L of 80% (v/v) MeOH containing 2.5 $\mu$M lidocaine and 10-camphor sulfonic acid per mg dry weight using a mixer mill with zirconia beads for 7 min at 18 Hz and 4°C. After centrifugation for 10 min, the supernatant was filtered using an HLB $\mu$Elution plate (Waters).

## LC-QTOF-MS Method

The extracts (1 $\mu$L) were analyzed using LC-QTOF-MS (LC, Waters Acquity UPLC system; MS, Waters Xevo G2 Q-Tof). Analytical conditions were as follows LC: column, Acquity bridged ethyl hybrid C18 (1.7 $\mu$m, 2.1 mm × 100 mm; Waters); solvent system, solvent A (water including 0.1% [v/v] formic acid) and solvent B (acetonitrile including 0.1% [v/v] formic acid); gradient program, 99.5% A/0.5% B at 0 min, 99.5% A/0.5% B at 0.1 min, 20% A/80% B at 10 min, 0.5% A/99.5% B at 10.1 min, 0.5% A/99.5% B at 12.0 min, 99.5% A/0.5% B at 12.1 min, and 99.5% A/0.5% B at 15.0 min; flow rate, 0.3 mL/min at 0 min, 0.3 mL/min at 10 min, 0.4 mL/min at 10.1 min, 0.4 min/min at 14.4 min, and 0.3 mL/min at 14.5 min; column temperature, 40°C; MS detection: capillary voltage, +3.00 kV (positive)/−2.75 kV (negative); cone voltage, 25.0 V, source temperature, 120°C, desolvation temperature, 450°C, cone gas flow, 50 L/h; desolvation gas flow, 800 L/h; collision energy, 6 V; mass range, $m/z$ 50–1500; scan duration, 0.1 s; interscan delay, 0.014 s; data acquisition, centroid mode; polarity, positive/negative; Lockspray (Leu enkephalin): scan duration, 1.0 s; and interscan delay, 0.1-s tandem mass spectrometry (MS/MS) data were acquired in the ramp mode as the following analytical conditions: (1) MS: mass range, $m/z$ 50–1500; scan duration, 0.1 s; interscan delay, 0.014 s; data acquisition, centroid mode; and (2) MS/MS: mass range, $m/z$ 50–1500; scan duration, 0.02 s; interscan delay, 0.014 s; data acquisition, centroid mode; polarity, negative collision energy, ramped from 10 to 50 V. In this mode, MS/MS spectra of the top 10 ions (>1000 counts) in an MS scan were automatically obtained. If the ion intensity was <1000, MS/MS data acquisition was not performed, and was moved to the next top-10 ions.

## LC-QTOF-MS Analysis

Data acquisition was performed using the software MassLynx 4.1 (Waters). Peaks of intensity <500 (noise level) were restored to 500. The peak intensity of the internal standard (10-camphor sulfonic acid) was used for normalization.

In each record, the list of exact mass was obtained from the KNApSAcK database (*Oryza* metabolites; Afendi et al., 2012) and Nakanishi et al. (1985), Rank et al. (2004), Huang et al. (2010), Kim et al. (2010), Huang et al. (2013), Zou et al. (2013), Yang et al. (2014), and Kusano et al. (2015). Values of $m/z$ were set as monoisotopic mass ([M+H]+ or [M-H]-), and searched for the value that the references and KNApSAcK matched with a tolerance of 0.01 D. For 36 specialized metabolites (Yang et al., 2014), values of retention time and $m/z$ were searched for matches with a tolerance of 0.2 min and 0.01 D, respectively.

## MS/MS

In MS/MS, an ion (precursor ion) is cleaved to many ions (product ions) by collision energy. More-reliable chemical assignment was performed using fragment pattern of reference. We compared MS/MS data in this project with previously published MS/MS data (Yang et al., 2014) to obtain exact mass.

## Pyrolysis-GCMS

The samples were ground into a fine powder by using an Automill (TK-AM7; Tokken) at 1,350 rpm for 5 min, washed with 100% methanol at 50°C for 5 min three times, and then washed again with Milli-Q water (Millipore) at 50°C for 5 min three more times. They were then completely dried out using a vacuum centrifuge (Sakuma Seisakusho) overnight. One mg of each sample powder was suspended in 1 mL of 100% (v/v) ethanol and 40 $\mu$L of this suspension (40 $\mu$g) was applied to the pyrolysis sheets. Pyrolysis-GCMS analysis was carried out under the following conditions: The sample was pyrolyzed with a Curie Point Pyrolyzer JPS-900 (automated model; Japan Analytical Industry) at 700°C (>50°C/ms) for 10 s using helium as the carrier gas with a mean linear velocity of 1 mL/min. The pyrolyzed sample was applied onto the column (ID 0.25 mm × Length 60 m × Film 0.25 $\mu$m; Agilent) fitted in an Agilent 6890A set without the split. The temperature of GC was held at 40°C for 1 min to trap and focus the volatile components, then programmed to a final temperature of 280°C at 4°C/min. Eluting compounds were detected with a mass spectrometer (JMS-AMSUN200, Benchtop QMS; JEOL), and the obtained mass spectrograms were collected at between 10 and 66 min.

## Thioglycolic Acid Lignin Assay, Thioacidolysis, and 2D-NMR

Rice root CWR samples used for thioglycolic acid assay and thioacidolysis were prepared as described in Cui et al. (2018). For 2D NMR analysis, CWRs were further subjected to acetylation in a dimethyl sulfoxide/*N*-methylimidazole/acetic anhydride system as described in Tobimatsu et al. (2013). The obtained acetylated CWRs (~15 mg) were dissolved in 600 $\mu$L of chloroform-*d* and subjected to NMR analysis. Thioglycolic acid lignin assay and thioacidolysis on CWRs were performed according to the methods described in Lam et al. (2017). NMR spectra were acquired on an Avance III 800US spectrometer (Bruker Biospin) fitted with a cryogenically cooled 5-mm TCI gradient probe. Adiabatic heteronuclear single quantum coherence NMR experiments on acetylated CWRs were carried out using standard implementation (hsqcetgpsp.3; Bruker Biospin) with parameters described in the literature (Wagner et al., 2011), and data processing and analysis were as described in Tobimatsu et al. (2013) and .

## RNA Extraction, cDNA Synthesis, and qPCR

Root RNA extraction and DNaseI treatment were performed as described in Mutuku et al. (2015). Briefly, root RNA extraction and DNaseI treatment used the RNeasy Plant Mini Kit (Qiagen) and Qiagen DNaseI solution following the manufacturer's instructions. The NanoDrop spectrophotometer (NanoDrop Technologies) was used to measure RNA concentration and purity. The ReverTra Ace qPCR Reverse Transcriptase kit (Toyobo) was used for first-strand cDNA synthesis. Into 35 ng of total RNA, 5× RT buffer, RT enzyme mix, and primer mix were added and incubated at 37°C for 15 min followed by 98°C for 5 min using the C1000 Thermal Cycler (Bio-Rad). The mixture was then diluted 10 times and stored at −20°C until use. qPCR was performed using Thunderbird SYBR qPCR mix (Toyobo). The reaction mixture of 20 $\mu$L total contained 2 $\mu$L of template cDNA, 10 $\mu$L of SYBR qPCR mix, 0.04 $\mu$L of 50× ROX Reference Dye (Thermo Fisher Scientific), 0.6 $\mu$L each of the forward and reverse primers, and 6.76 $\mu$L of distilled autoclaved water. All qPCRs were performed in three technical replicates, and three independent biological replicates were analyzed. MX3000P (Stratagene) was used to perform qPCR and the data were analyzed using the software MXPro QPCR 4.10d (Stratagene). qPCR was performed in three segments. Segment 1 consisted of 15 min at 95°C for one cycle, segment 2 consisted of 15 s at 95°C and 30 s at 60°C for 40 cycles, and segment 3 consisted of 1 min at 95°C, 30 s at 55°C, and 30 s at 95°C for one cycle. Data were obtained and transferred to the program Excel (Microsoft) for further handling. Gene expression was normalized using *OsCyclophilin* (Mutuku et al., 2015). Statistically significant induction was determined by comparing gene expression at 1, 3, and 7 dpi with that at 0 dpi (uninfected control). Supplemental Table S1 shows the description of target genes used in this study and the primer pairs used for qPCR.

## Data Analysis

Statistical analysis (Student's *t* test) was done using GraphPad Prism version 7.0 (GraphPad Software; www.graphpad.com).

## Accession Numbers

Accession numbers, sequences, and references have been given in Supplemental Table S1.

## Supplemental Data

The following supplemental materials are available.

**Supplemental Figure S1.** Untargeted profiling using LC-Q-TOF-MS positive ion mode of control, *S. hermonthica*-infected rice, and that of *S. hermonthica* radicles at 4 d after induction of germination by strigol.

**Supplemental Figure S2.** Lignin composition in the roots of Nipponbare with reduced *C3′H* expression.

**Supplemental Table S1.** The description of target genes used in this study and the primer pairs used for RT-qPCR.

**Supplemental Data Set S1.** Untargeted profiling using LC-Q-TOF-MS negative ion mode of control, *S. hermonthica*-infected rice, and that of *S. hermonthica* radicles at 4 d after induction of germination by strigol.

**Supplemental Data Set S2.** Untargeted profiling using LC-Q-TOF-MS positive ion mode of control, *S. hermonthica*-infected rice, and that of *S. hermonthica* radicles at 4 d after induction of germination by strigol.

**Supplemental Data Set S3.** Lignin-derived, carbohydrate-derived, and other compounds identified in pyrolysis-GCMS.

## ACKNOWLEDGMENTS

We thank Alpha Kamara and Mel Oluoch (International Institute of Tropical Agriculture) for providing *S. hermonthica* seeds, Professor Kenji Mori for providing strigol, and Dr. Hironori Kaji and Ms. Ayaka Maeno (Kyoto University) for their support in the NMR experiments. A part of this study was conducted using the facilities in the Development and Assessment of Sustainable Humanosphere (DASH)/ Forest Biomass Analytical System (FBAS) at the Research Institute for Sustainable Humanosphere (RISH), Kyoto University, and the NMR spectrometer in the Joint Usage/Research Center (JURC) at the Institute for Chemical Research (ICR), Kyoto University.

Received September 24, 2018; accepted January 13, 2019; published January 22, 2019.

## LITERATURE CITED

**Abdulrazzak N, Pollet B, Ehlting J, Larsen K, Asnaghi C, Ronseau S, Proux C, Erhardt M, Seltzer V, Renou JP, et al** (2006) A coumaroyl-ester-3-hydroxylase insertion mutant reveals the existence of nonredundant meta-hydroxylation pathways and essential roles for phenolic precursors in cell expansion and plant growth. Plant Physiol **140:** 30–48

**Afendi FM, Okada T, Yamazaki M, Hirai-Morita A, Nakamura Y, Nakamura K, Ikeda S, Takahashi H, Altaf-Ul-Amin M, Darusman LK, et al** (2012) KNApSAcK family databases: Integrated metabolite-plant species databases for multifaceted plant research. Plant Cell Physiol **53:** e1

**Becerra-Moreno A, Redondo-Gil M, Benavides J, Nair V, Cisneros-Zevallos L, Jacobo-Velázquez DA** (2015) Combined effect of water loss and wounding stress on gene activation of metabolic pathways associated with phenolic biosynthesis in carrot. Front Plant Sci **6:** 837

**Bhuiyan NH, Selvaraj G, Wei Y, King J** (2009) Gene expression profiling and silencing reveal that monolignol biosynthesis plays a critical role in penetration defence in wheat against powdery mildew invasion. J Exp Bot **60:** 509–521

**Bonawitz ND, Kim JI, Tobimatsu Y, Ciesielski PN, Anderson NA, Ximenes E, Maeda J, Ralph J, Donohoe BS, Ladisch M, et al** (2014) Disruption of Mediator rescues the stunted growth of a lignin-deficient *Arabidopsis* mutant. Nature **509:** 376–380

**Caño-Delgado A, Penfield S, Smith C, Catley M, Bevan M** (2003) Reduced cellulose synthesis invokes lignification and defense responses in *Arabidopsis thaliana*. Plant J **34:** 351–362

**Cass CL, Peraldi A, Dowd PF, Mottiar Y, Santoro N, Karlen SD, Bukhman YV, Foster CE, Thrower N, Bruno LC, et al** (2015) Effects of PHENYLALANINE AMMONIA LYASE (PAL) knockdown on cell wall composition, biomass digestibility, and biotic and abiotic stress responses in Brachypodium. J Exp Bot **66:** 4317–4335

**Cissoko M, Boisnard A, Rodenburg J, Press MC, Scholes JD** (2011) New Rice for Africa (NERICA) cultivars exhibit different levels of post-attachment resistance against the parasitic weeds *Striga hermonthica* and *Striga asiatica*. New Phytol **192:** 952–963

**Cui S, Wakatake T, Hashimoto K, Saucet SB, Toyooka K, Yoshida S, Shirasu K** (2016) Haustorial hairs are specialized root hairs that support parasitism in the facultative parasitic plant *Phtheirospermum japonicum*. Plant Physiol **170:** 1492–1503

**Cui S, Wada S, Tobimatsu Y, Takeda Y, Saucet SB, Takano T, Umezawa T, Shirasu K, Yoshida S** (2018) Host lignin composition affects haustorium induction in the parasitic plants *Phtheirospermum japonicum* and *Striga hermonthica*. New Phytol **218:** 710–723

**del Río JC, Rencoret J, Prinsen P, Martínez ÁT, Ralph J, Gutiérrez A** (2012) Structural characterization of wheat straw lignin as revealed by analytical pyrolysis, 2D-NMR, and reductive cleavage methods. J Agric Food Chem **60:** 5922–5935

**Dong X, Chen W, Wang W, Zhang H, Liu X, Luo J** (2014) Comprehensive profiling and natural variation of flavonoids in rice. J Integr Plant Biol **56:** 876–886

**Faix O, Meier D, Fortmann I** (1990) Thermal degradation products of wood: Gas chromatographic separation and mass spectrometric characterization of monomeric lignin-derived products. Eur J Wood Wood Prod **48:** 281–285.

**Faix O, Fortmann I, Bremer J, Meier J** (1991) Thermal degradation products of wood: A collection of electron-impact (EI) mass spectra of polysaccharide-derived products. Eur J Wood Wood Prod **49:** 299–304.

**Franke R, Hemm MR, Denault JW, Ruegger MO, Humphreys JM, Chapple C** (2002) Changes in secondary metabolism and deposition of an unusual lignin in the *ref8* mutant of *Arabidopsis*. Plant J **30:** 47–59

**Funnell-Harris DL, Pedersen JF, Sattler SE** (2010) Alteration in lignin biosynthesis restricts growth of *Fusarium* spp. in brown midrib sorghum. Phytopathology **100:** 671–681

**Gallego-Giraldo L, Jikumaru Y, Kamiya Y, Tang Y, Dixon RA** (2011) Selective lignin downregulation leads to constitutive defense response expression in alfalfa (*Medicago sativa* L.). New Phytol **190:** 627–639

**Gobena D, Shimels M, Rich PJ, Ruyter-Spira C, Bouwmeester H, Kanuganti S, Mengiste T, Ejeta G** (2017) Mutation in sorghum *LOW GERMINATION STIMULANT 1* alters strigolactones and causes *Striga* resistance. Proc Natl Acad Sci USA **114:** 4471–4476

**Gui J, Shen J, Li L** (2011) Functional characterization of evolutionarily divergent 4-coumarate: Coenzyme a ligases in rice. Plant Physiol **157:** 574–586

**Gunnaiah R, Kushalappa AC, Duggavathi R, Fox S, Somers DJ** (2012) Integrated metabolo-proteomic approach to decipher the mechanisms by which wheat QTL (Fhb1) contributes to resistance against *Fusarium graminearum*. PLoS One **7:** e40695

**Gurney AL, Slate J, Press MC, Scholes JD** (2006) A novel form of resistance in rice to the angiosperm parasite *Striga hermonthica*. New Phytol **169:** 199–208

**Harahap Z, Ampongnyarko K, Olela J** (1993) *Striga hermonthica* resistance in upland rice. Crop Prot **12:** 229–231

**Hess D, Ejeta G, Butler L** (1992) Selecting sorghum genotypes expressing a quantitative biosynthetic trait that confers resistance to *Striga*. Phytochemistry **31:** 493–497

**Hirayama K, Mori K** (1999) Synthesis of (+)-Strigol and (+)-Orobanchol, the germination stimulants, and their stereoisomers by employing lipase-catalyzed asymmetric acetylationas the key step. Eur J Org Chem **1999:** 2211–2217

**Hoffmann L, Besseau S, Geoffroy P, Ritzenthaler C, Meyer D, Lapierre C, Pollet B, Legrand M** (2004) Silencing of hydroxycinnamoyl-coenzyme A shikimate/quinate hydroxycinnamoyltransferase affects phenylpropanoid biosynthesis. Plant Cell **16:** 1446–1465

**Huang S, Chen JH, Gong M, Huang MQ, Li J, Wu AG, Lai XP** (2010) [Studies on the flavonoids from the herb of *Striga asiatica*.] [in Chinese] Zhong Yao Cai **33:** 1089–1091

**Huang W, Wu SB, Wang YL, Guo ZY, Kennelly EJ, Long CL** (2013) Chemical constituents from *Striga asiatica* and its chemotaxonomic study. Biochem Syst Ecol **48:** 100–106

**Humphreys JM, Chapple C** (2002) Rewriting the lignin roadmap. Curr Opin Plant Biol **5:** 224–229

**Jamil M, Rodenburg J, Charnikhova T, Bouwmeester HJ** (2011) Pre-attachment *Striga hermonthica* resistance of New Rice for Africa (NERICA) cultivars based on low strigolactone production. New Phytol **192:** 964–975

**Jones M, Dingkuhn M, Aluko G, Semon M** (1997) Interspecific *Oryza sativa* L. X *O. Glaberrima* Steud. progenies in upland rice improvement. Euphytica **92:** 237–246

**Kim H, Kim D, Jang Y** (2010) Phytochemical analysis of *Striga hermonthica* by DART-MS and HPLC-MS. Planta Med **76:** P217

**König S, Feussner K, Kaever A, Landesfeind M, Thurow C, Karlovsky P, Gatz C, Polle A, Feussner I** (2014) Soluble phenylpropanoids are involved in the defense response of Arabidopsis against *Verticillium longisporum*. New Phytol **202:** 823–837

**Koshiba T, Hirose N, Mukai M, Yamamura M, Hattori T, Suzuki S, Sakamoto M, Umezawa T** (2013) Characterization of 5-hydroxyconiferaldehyde O-methyltransferase in *Oryza sativa*. Plant Biotechnol **30:** 157–167

**Kusano M, Yang Z, Okazaki Y, Nakabayashi R, Fukushima A, Saito K** (2015) Using metabolomic approaches to explore chemical diversity in rice. Mol Plant **8:** 58–67

**Kusumoto D, Goldwasser Y, Xie X, Yoneyama K, Takeuchi Y, Yoneyama K** (2007) Resistance of red clover (*Trifolium pratense*) to the root parasitic plant *Orobanche minor* is activated by salicylate but not by jasmonate. Ann Bot **100:** 537–544

**Labrousse P, Arnaud M, Serieys H, Berville A, Thalouarn P** (2001) Several mechanisms are involved in resistance of *Helianthus* to *Orobanche cumana* Wallr. Ann Bot **88:** 859–868

**Lam PY, Tobimatsu Y, Takeda Y, Suzuki S, Yamamura M, Umezawa T, Lo C** (2017) Disrupting flavone synthase II alters lignin and improves biomass digestibility. Plant Physiol **174:** 972–985

**Lan W, Lu F, Regner M, Zhu Y, Rencoret J, Ralph SA, Zakai UI, Morreel K, Boerjan W, Ralph J** (2015) Tricin, a flavonoid monomer in monocot lignification. Plant Physiol **167:** 1284–1295

**Li J, Timko MP** (2009) Gene-for-gene resistance in *Striga*-cowpea associations. Science **325:** 1094

**Li M, Foster C, Kelkar S, Pu Y, Holmes D, Ragauskas A, Saffron CM, Hodge DB** (2012) Structural characterization of alkaline hydrogen peroxide pretreated grasses exhibiting diverse lignin phenotypes. Biotechnol Biofuels **5:** 38

**Lu Q, Tian H-Y, Hu B, Jiang X-Y, Dong C-Q, Yang Y-P** (2016) Pyrolysis mechanism of holocellulose-based monosaccharides: The formation of hydroxyacetaldehyde. J Anal Appl Pyrolysis **120:** 15–26

**Matusova R, Rani K, Verstappen FW, Franssen MC, Beale MH, Bouwmeester HJ** (2005) The strigolactone germination stimulants of the plant-parasitic *Striga* and *Orobanche* spp. are derived from the carotenoid pathway. Plant Physiol **139:** 920–934

**Maury S, Delaunay A, Mesnard F, Crônier D, Chabbert B, Geoffroy P, Legrand M** (2010) O-methyltransferase(s)-suppressed plants produce lower amounts of phenolic vir inducers and are less susceptible to *Agrobacterium tumefaciens* infection. Planta **232:** 975–986

**Moghaddam L, Rencoret J, Maliger V, Rackemann D, Harrison M, Gutierrez A, del Río J, Doherty W** (2017) Structural characteristics of bagasse furfural residue and its lignin component. An NMR, Py-GC/MS, and FTIR study. ACS Sustain Chem Eng **5:** 4846–4855

**Mutuku JM, Nose A** (2012) Changes in the contents of metabolites and enzyme activities in rice plants responding to *Rhizoctonia solani* Kuhn infection: Activation of glycolysis and connection to phenylpropanoid pathway. Plant Cell Physiol **53:** 1017–1032

**Mutuku JM, Yoshida S, Shimizu T, Ichihashi Y, Wakatake T, Takahashi A, Seo M, Shirasu K** (2015) The WRKY45-dependent signaling pathway is required for resistance against *Striga hermonthica* parasitism. Plant Physiol **168:** 1152–1163

**Nakanishi T, Ogaki J, Inada A, Murata H, Nishi M, Iinuma M, Yoneda K** (1985) Flavonoids of *Striga asiatica*. J Nat Prod **48:** 491–493

**Oliver L, Pedersen F, Grant J, Klopfenstein J, Jose H** (2005) Comparative effects of the sorghum bmr-6 and bmr-12 genes. I. Grain yield, stover yield, and stover quality in grain sorghum. Crop Sci **45:** 2240–2245

**Pattathil S, Hahn MG, Dale BE, Chundawat SP** (2015) Insights into plant cell wall structure, architecture, and integrity using glycome profiling of native and AFEXTM-pre-treated biomass. J Exp Bot **66:** 4279–4294

**Ralph J, Hatfield R** (1991) Pyrolysis-GC-MS characterization of forage materials. J Agric Food Chem **39:** 1426–1437

**Ralph J, Akiyama T, Kim H, Lu F, Schatz PF, Marita JM, Ralph SA, Reddy MS, Chen F, Dixon RA** (2006) Effects of coumarate 3-hydroxylase down-regulation on lignin structure. J Biol Chem **281:** 8843–8853

**Rank C, Rasmussen LS, Jensen SR, Pierce S, Press MC, Scholes JD** (2004) Cytotoxic constituents of *Alectra* and *Striga* species. Weed Res **44:** 265–270

**Riches C, Parker C** (1995) Parasitic plants as weeds. *In* M Press and J Graves, eds, Parasitic Plants. Chapman and Hall, London, pp 226–255

**Rodenburg J, Cissoko M, Kayeke J, Dieng I, Khan Z, Midega C, Onyuka E, Scholes J** (2015) Do NERICA rice cultivars express resistance to *Striga hermonthica* (Del.) Benth. and *Striga asiatica* (L.) Kuntze under field conditions? Field Crops Res **170:** 83–94

**Saucet SB, Shirasu K** (2016) Molecular parasitic plant–host interactions. PLoS Pathog **12:** e1005978

**Scholes JD, Press MC** (2008) *Striga* infestation of cereal crops—an unsolved problem in resource limited agriculture. Curr Opin Plant Biol **11:** 180–186

**Spallek T, Mutuku M, Shirasu K** (2013) The genus Striga: A witch profile. Mol Plant Pathol **14:** 861–869

**Spallek T, Melnyk CW, Wakatake T, Zhang J, Sakamoto Y, Kiba T, Yoshida S, Matsunaga S, Sakakibara H, Shirasu K** (2017) Interspecies hormonal control of host root morphology by parasitic plants. Proc Natl Acad Sci USA **114:** 5283–5288

**Swarbrick PJ, Huang K, Liu G, Slate J, Press MC, Scholes JD** (2008) Global patterns of gene expression in rice cultivars undergoing a susceptible or resistant interaction with the parasitic plant *Striga hermonthica*. New Phytol **179:** 515–529

**Takeda Y, Koshiba T, Tobimatsu Y, Suzuki S, Murakami S, Yamamura M, Rahman MM, Takano T, Hattori T, Sakamoto M, et al** (2017) Regulation of CONIFERALDEHYDE 5-HYDROXYLASE expression to modulate cell wall lignin structure in rice. Planta **246:** 337–349

**Takeda Y, Tobimatsu Y, Karlen SD, Koshiba T, Suzuki S, Yamamura M, Murakami S, Mukai M, Hattori T, Osakabe K, et al** (2018) Down-regulation of *p*-COUMAROYL ESTER 3-HYDROXYLASE in rice leads to altered cell wall structures and improves biomass saccharification. Plant J **95:** 796–811

**Tobimatsu Y, Chen F, Nakashima J, Escamilla-Treviño LL, Jackson L, Dixon RA, Ralph J** (2013) Coexistence but independent biosynthesis of catechyl and guaiacyl/syringyl lignin polymers in seed coats. Plant Cell **25:** 2587–2600

**Vanholme R, Storme V, Vanholme B, Sundin L, Christensen JH, Goeminne G, Halpin C, Rohde A, Morreel K, Boerjan W** (2012) A systems biology view of responses to lignin biosynthesis perturbations in Arabidopsis. Plant Cell **24:** 3506–3529

**Verhage A, van Wees SC, Pieterse CM** (2010) Plant immunity: It's the hormones talking, but what do they say? Plant Physiol **154:** 536–540

**Vermerris W, Sherman DM, McIntyre LM** (2010) Phenotypic plasticity in cell walls of maize brown midrib mutants is limited by lignin composition. J Exp Bot **61:** 2479–2490

**Wagner A, Tobimatsu Y, Phillips L, Flint H, Torr K, Donaldson L, Pears L, Ralph J** (2011) CCoAOMT suppression modifies lignin composition in *Pinus radiata*. Plant J **67:** 119–129

**Yang Z, Nakabayashi R, Okazaki Y, Mori T, Takamatsu S, Kitanaka S, Kikuchi J, Saito K** (2014) Toward better annotation in plant metabolomics: Isolation and structure elucidation of 36 specialized metabolites from *Oryza sativa* (rice) by using MS/MS and NMR analyses. Metabolomics **10:** 543–555

**Yoshida S, Shirasu K** (2009) Multiple layers of incompatibility to the parasitic witchweed, *Striga hermonthica*. New Phytol **183:** 180–189

**Yoshida S, Cui S, Ichihashi Y, Shirasu K** (2016) The haustorium, a specialized invasive organ in parasitic plants. Annu Rev Plant Biol **67:** 643–667

**Zhang K, Qian Q, Huang Z, Wang Y, Li M, Hong L, Zeng D, Gu M, Chu C, Cheng Z** (2006) GOLD HULL AND INTERNODE2 encodes a primarily multifunctional cinnamyl-alcohol dehydrogenase in rice. Plant Physiol **140:** 972–983

**Zou YS, Foubert K, Tuenter E, Lemière F, Cos P, Maes L, Smits JMM, Gelder R, Apers S, Pieters L** (2013) Antiplasmodial and cytotoxic activities of *Striga asiatica* and *Sauropus spatulifolius* extracts, and their isolated constituents. Phytochem Lett **6:** 53–58